

and the sound absorption coefficient is equal to

$$\frac{\Gamma_{\max}}{\omega} = \frac{k''s}{\omega} = \gamma \frac{\omega c^2}{8\pi s^2 \sigma_{zz}} \alpha \frac{1}{(\sqrt{|\Omega|}) + \kappa \varphi^2 |g_0|}. \quad (6.12)$$

The result (6.12) agrees with the behavior of the experimental curve $\Gamma_{\max}(\varphi)$ on Fig. 9.

¹There is no corresponding value $(2\pi\hbar)^{-1}(\partial S/\partial p_H) \approx 1.5$ of the known model of the Fermi surface of W (Ref. 16).

²This value of the concentration in molybdenum agrees with the value of n_0 given in Ref. 18.

³The influence of the magnetic damping on the dopplerons in Cd was investigated in Ref. 20.

⁴A. A. Galkin, L. T. Tsymbal, T. F. Butenko, A. N. Cherkasov, and A. M. Grishin, Phys. Lett. **67A**, 207 (1978).

⁵L. M. Fisher, V. V. Lavrova, V. A. Yudin, O. V. Konstantinov, and V. G. Skobov, Zh. Eksp. Teor. Fiz. **60**, 759 (1971); **63**, 224 (1972) [Sov. Phys. JETP **33**, 410 (1971); **36**, 118 (1972)].

⁶V. P. Naberezhnykh, D. E. Zherebchevskii, L. T. Tsymbal, and T. M. Yeryomenko, Solid State Commun. **11**, 1529 (1972).

⁷D. S. Falk, B. Gerson, and J. F. Carolan, Phys. Rev. B **1**, 406 (1970).

⁸W. M. Lomer, Proc. Phys. Soc. London **80**, 489 (1962); **84**, 327 (1964).

⁹V. A. Gasparov and M. H. Harutunian, Phys. Status Solidi B **93**, 403 (1979).

¹⁰D. E. Soule and J. C. Abele, Phys. Rev. Lett. **23**, 1287 (1969).

¹¹L. T. Tsymbal, Yu. D. Samokhin, A. N. Cherkasov, V. T. Vitchinkin, and V. A. Mishin, Fiz. Nizk. Temp. **5**, 461 (1979)

[Sov. J. Low Temp. Phys. **5**, 221 (1979)].

¹²P. D. Hambourger and J. A. Marcus, Phys. Rev. B **8**, 5567 (1973).

¹³L. T. Tsymbal and T. F. Butenko, Solid State Commun. **13**, 633 (1973).

¹⁴A. A. Galkin, L. T. Tsymbal, A. M. Grishin, and T. F. Butenko, Pis'ma Zh. Eksp. Teor. Fiz. **25**, 98 (1977) [JETP Lett. **25**, 87 (1977)].

¹⁵V. F. Gantmacher, Prog. Low Temp. Phys. **5**, 181 (1967).

¹⁶H. J. McScimin, J. Acoust. Soc. Am. **22**, 413 (1950).

¹⁷I. M. Vitebskii, V. T. Vitchinkin, A. A. Galkin, Yu. A. Ostroukhov, O. A. Panchenko, L. T. Tsymbal, and A. N. Cherkasov, Fiz. Nizk. Temp. **1**, 400 (1975) [Sov. J. Low Temp. Phys. **1**, 200 (1975)].

¹⁸A. A. Galkin, L. T. Tsymbal, A. N. Cherkasov, and I. M. Vitebskii, Fiz. Nizk. Temp. **1**, 540 (1975) [Sov. J. Low Temp. Phys. **1**, 264 (1975)].

¹⁹J. B. Ketterson, D. D. Koelling, J. C. Shaw, and L. R. Windmiller, Phys. Rev. B **11**, 1447 (1975).

²⁰V. P. Naberezhnykh, A. A. Mar'yakhin, and V. L. Mel'nik, Zh. Eksp. Teor. Fiz. **52**, 617 (1967) [Sov. Phys. JETP **25**, 403 (1967)].

²¹V. V. Boiko, V. A. Gasparov, and I. G. Gverdtsiteli, Zh. Eksp. Teor. Fiz. **56**, 489 (1969) [Sov. Phys. JETP **29**, 269 (1969)].

²²E. A. Kaner and V. G. Skobov, Adv. Phys. **17**, 605 (1968).

²³V. V. Lavrova, V. G. Skobov, L. M. Fisher, A. S. Chernov, and V. A. Yudin, Fiz. Tverd. Tela (Leningrad) **15**, 2335 (1973) [Sov. Phys. Solid State **15**, 1558 (1973)].

²⁴S. V. Medvedev, V. G. Skobov, L. M. Fisher, and V. A. Yudin, Zh. Eksp. Teor. Fiz. **69**, 2267 (1975) [Sov. Phys. JETP **42**, 1152 (1975)].

Translated by J. G. Adashko

Investigation of the band structure of semiconducting Bi_{1-x}Sb_x alloys

G. A. Mironova, M. V. Sudakova, and Ya. G. Ponomarev

Moscow State University

(Submitted 26 July 1979)

Zh. Eksp. Teor. Fiz. **78**, 1830-1851 (May 1980)

The Shubnikof-de Haas effect is investigated at helium temperatures in the semiconducting alloys Bi_{1-x}Sb_x (0.08 ≤ x ≤ 0.12) of both n and p type. It is observed that the anisotropy of the electron (n-type) and hole (p-type) Fermi surfaces at the point L of the reduced Brillouin zone decreases with increasing Fermi energy ε_F. The difference between the anisotropic cross sections and the cyclotron masses increases simultaneously. The degree of nonspecularity of the electron and hole spectra in the direction of elongation of the equal-energy surfaces in L is determined. It is observed that the ratio of the spin and orbit splittings γ = Δ_{sp}/Δ_{orb} for the maximum section of the Fermi surface in L(H||C₂) approaches unity as ε_F → 0. The parameters that enter in McClure's dispersion relation [J. Low Temp. Phys. **25**, 527 (1976)] are calculated.

PACS numbers: 71.25.Tn, 72.20.Mg, 71.25.Hc

INTRODUCTION

The restructuring of the energy spectrum of Bi_{1-x}Sb_x with increasing x is accompanied by a transition of the alloys into the superconducting phase in a relatively narrow concentration interval 0.07 < x < 0.23.¹ The thermal gap of the semiconducting alloys Bi_{1-x}Sb_x does not exceed 25-30 meV, so that they can be classified as

narrow-gap semiconductors.^{1,2} According to the results of magneto-optical measurements,³ the energy gap ε_{gL} at the point L of the reduced Brillouin zone vanishes at x ≈ 0.04 as a result of the band inversion (the gap parameter of Bi is ε_{gL} < 0). The anomalous smallness of the direct gap ε_{gL} leads to a strong nonparabolicity of the dispersion of the carriers in L.⁴⁻¹⁰

The experimental data¹¹ obtained for pure Bi are best

described by the dispersion relation proposed by McClure and Choi,¹⁰ In a simplified version, the McClure dispersion law is of the form⁹

$$\left[\varepsilon + \frac{\alpha_v - \alpha_c}{2} \frac{k_y^2}{2} \right]^2 = \left[\frac{\varepsilon_{gL}}{2} + \frac{\alpha_v + \alpha_c}{2} \frac{k_y^2}{2} \right]^2 + Q_{11}^2 k_x^2 + Q_{22}^2 k_y^2 + Q_{33}^2 k_z^2, \quad (1)$$

where ε is the energy reckoned from the center of the gap, and \mathbf{k} is the wave vector; the x axis coincides with the binary C_2 axis and y with the direction of elongation of the equal-energy surface in L . Q_{ii} are the counterparts of the Kane matrix elements, and α_c and α_v are longitudinal reciprocal corrections masses for the electrons and holes respectively; they appear when account is taken of the interaction with the more remote bands in the y direction. The quantities in (1) are expressed in atomic units (the energy in Hartree units, where 1 Hartree is equal to 2 Ry, and the distances are in Bohr radii).

Equation (1) goes over into the Lax dispersion law⁴ at $\alpha_c = \alpha_v = 0$, and into the dispersion law of Abrikosov⁸ or Cohen⁵ (we have in mind here the simplified Cohen model) at $Q_{22} = 0$. The Lax model,⁴ which takes into account the interaction of only two most closely located bands in L , is in qualitative contradiction with a number of experimental results and is incapable, in particular, of explaining the growth of the anisotropy of the equal-energy surfaces in L following inversion of the bands under pressure¹² in the semiconducting alloys $\text{Bi}_{1-x}\text{Sb}_x$, and the decrease of the anisotropy with increasing Fermi energy.¹³

A distinguishing feature of the models of Abrikosov⁸ and Cohen⁵ is the existence of two stable points of tangency of the conduction band and the valence band at negative values of the gap parameter ε_{gL} . The absence of such points is indicated by the experimental data.^{14,15} It should be noted that the appearance of the parameter Q_{22} in the dispersion law (1) lifts the band degeneracy at the indicated points at $\varepsilon_{gL} < 0$, from which follows that this parameter is of principal importance (even if it is small).

Let us dwell in greater detail on the characteristic features of the band spectrum described by relation (1):

- 1) The equal-energy surfaces, strictly speaking, are not ellipsoidal (owing to the presence of terms $\sim k_y^4$).
- 2) The dispersion laws of the electrons and holes in the elongation direction (y) are in the general case non-specular (specularity is possible only at $\alpha_v = \alpha_c$).
- 3) The anisotropy of the equal-energy surfaces and of the cyclotron masses of the carriers in L coincide only at the bottom (top) of the bands and depend both on the Fermi energy ε_F and on ε_{gL} .
- 4) The gap dependences of the anisotropies of the equal-energy surfaces and of the cyclotron masses of the carriers in L are asymmetric with respect to $\varepsilon_{gL} = 0$.
- 5) At negative values of the gap parameter and at $\alpha_c, \alpha_v > 0$, the point L becomes a saddle point in the electron and hole spectrum at $\varepsilon_{gL}^* = -2Q_{22}^2/\alpha_v$ and $\varepsilon_{gL}^{**} = -2Q_{22}^2/\alpha_c$, respectively (on going through the gapless

state, the conduction and valence bands exchange the reciprocal correction masses α_v, α_c).

6) In the direction of the shorter semiaxis of the equal-energy surfaces in L , the dispersion relation (1) retains the Lax form (in contrast to the more complicated spectrum of McClure and Choi,¹⁰ in which account is taken of the interaction with the remote bands in the x and z directions). In the spectrum (1) the function $\varepsilon(\mathbf{k})$ in the x and z directions is symmetrical at the point L ($k_y = 0$) with respect to $\varepsilon_{gL} = 0$.

A dispersion relation of the type (1) for the superconducting alloys $\text{Bi}_{1-x}\text{Sb}_x$ was proposed by Antcliffe¹⁶ in 1969. He also cited data that point to a strong non-specularity of the electron and hole spectra in L in the y direction. Succeeding measurements¹⁷ have shown that the anisotropy obtained by Antcliffe¹⁶ for the hole Fermi surfaces of the alloy $p\text{-Bi}_{0.88}\text{Sb}_{0.12}$ in L turned out to be undervalued by a factor of 2.

A check on the applicability of the McClure model⁹ for semiconducting alloys $\text{Bi}_{1-x}\text{Sb}_x$ with a normal spectrum ($\varepsilon_{gL} > 0$) is of particular interest, since the parameters of the spectrum ($Q_{ii}, \alpha_c, \alpha_v$) can change in principle with increasing x . For a reliable determination of these parameters for an alloy with given x it is necessary to vary the Fermi energy ε_F in a wide range, both in conduction and in the valence band, by introducing into the alloy donor or acceptor impurities. The angular dependences of the cyclotron masses of the electrons and holes in L , for semiconducting alloys $\text{Bi}_{1-x}\text{Sb}_x$ with impurity carrier density $< 10^{16} \text{ cm}^{-3}$ were investigated in detail using cyclotron resonance.¹⁸⁻²⁰ A study of cyclotron resonance of $\text{Bi}_{1-x}\text{Sb}_x$ alloys with large electron or hole density at the presently available technique entails great difficulties (because of the relatively short relaxation time τ). The most efficient under these conditions is an investigation of the Shubnikov-de Haas (SdH) or of the de Haas-van Alphen (dHvA) effect at low temperatures; this yields the angular dependences of the extremal sections of the Fermi surfaces and of the cyclotron masses.^{13,16,17,21,22} The limitations on the carrier density in the latter case are connected mainly with the maximum fields that can be obtained in experiment.

Investigations of the SdH effect in $n\text{-Bi}_{1-x}\text{Sb}_x$ have shown¹³ that the interpretation of the oscillation curves is made difficult in some cases by the motion of the Fermi level in the magnetic field. Frequency modulation of the quantum oscillations of the magnetic susceptibility and of the magnetoresistance of Bi, which is connected with the motion of ε_F in the magnetic field, was investigated in Refs. 23-26. Calculation of $\varepsilon_F(H)$ of Bi at various orientations of the magnetic field relative to the crystallographic axes was carried out by Smith, Baraff, and Rowell (SBR) on the basis of a semi-empirical dispersion relation (a modified Lax dispersion law in a magnetic field)²³

$$\varepsilon = \frac{1}{2} \left\{ \varepsilon_{gL}^2 + 4\varepsilon_{gL} \left[\hbar\omega_c \left(n + \frac{1}{2} + \frac{s}{2} \gamma \right) + \frac{p_0^2}{2m_u} \right] \right\}^{1/2}, \quad (2)$$

where $\omega_c = eH/m_c^* c$ is the cyclotron frequency corresponding to the bottom of the band, m_u^* is the trans-

port mass at the bottom of the band in the direction of the magnetic field H , p_{\parallel} is the quasimomentum in the direction of the magnetic field H , $s = \pm 1$ is the spin quantum number, $\gamma = \Delta_s / \Delta_{orb} = m_c^* / m_s^*$ is the ratio of the spin splitting to the orbit splitting, and m_c^* and m_s^* are respectively the cyclotron and spin masses at the bottom of the band. The quantity m_c^* is expressed in terms of the components of the effective mass tensor \hat{m}^* on the bottom of the band:

$$m_c^* = [\det \hat{m}^* / m_{\parallel}^*]^{1/2}, \quad m_{\parallel}^* = \mathbf{g} \hat{m}^* \mathbf{g},$$

(\mathbf{g} is a unit vector in the magnetic-field direction).

Similarly, m_s^* is expressed in terms of the components of the spin mass \hat{m}_s^* .^{26, 27}

At $\gamma = m_c^* / m_s^* = 1$ relation (2) corresponds to the simple two-band model.²⁷ It follows from experiment, however, that in the case of Bi, even for the smallest cross section of the electron Fermi surface ($H \parallel y$), we have $\gamma \neq 1$ ($\gamma(H \parallel y) = 1.07$, $\gamma(H \parallel z) = 0.34$, $\gamma(H \parallel x) = 0.3$),^{26, 28, 29} The latter is patently the consequence of the influence of the remote bands on the energy spectrum of the carriers of Bi in L , so that the applicability of relation (2) at $\gamma \neq 1$ calls for a serious justification. Calculations performed by Baraff³⁰ have shown that in the case when the corrections for the interaction with the remote bands are small, relation (2) remains formally in force for all the Landau equations, with the exception of the levels with $n = 0$ and $s = 1$, under the condition that m_c^* and m_s^* are themselves now functions of the energy ε . In particular, it follows from this that γ is likewise independent of ε (Ref. 28), with $\gamma \rightarrow 1$ as $\varepsilon \rightarrow 0$ and $\varepsilon_{gL} \rightarrow 0$. It is clear from the foregoing that the components of the tensors \hat{m}^* and \hat{m}_s^* , determined within the framework of the SBR model in Ref. 26, characterize strictly speaking only the electrons on the Fermi level in pure bismuth, and should be redefined in the case of the alloys $\text{Bi}_{1-x}\text{Sb}_x$, $\text{Bi}_{1-x}\text{Te}_x$ and $\text{Bi}_{1-x}\text{Sn}_x$.

The effects connected with the motion of the Fermi level of Bi and of alloys on its basis in a magnetic field turn out to be particularly significant when quantum oscillations are observed simultaneously from several Fermi-surface sections that differ noticeably in size. In magnetic fields comparable with the quantum-limit field for the smallest section, the period of the oscillations $\Delta(1/H)$ from other sections is not a constant quantity, and can differ in a definite region of the magnetic fields from the value $\Delta(1/H)_{H \rightarrow 0} = eh/cS_{\text{extr}}$, corresponding to the condition $\varepsilon_F = \text{const}(S_{\text{extr}}$ is the extremal section of the Fermi surface in p -space).^{23-26, 13} In such cases, an exact determination of S_{extr} is impossible without a calculation of the function $\varepsilon_F(H)$.²⁶ Similar calculations are necessary for the determination of the true values^{28, 29} of γ and of the cyclotron masses of the carriers from the oscillation curves.

It should be noted that the effects connected with the motion of ε_F in a magnetic field become weaker when acceptor impurities (Sn, Pb) are introduced into the bismuth, inasmuch as in this case the stabilizing action of the hole extremum at the point T becomes stronger.³¹ Obviously, a similar picture should be observed in p - $\text{Bi}_{1-x}\text{Sb}_x$ semiconducting alloys.

In this paper we report detailed investigations of the SdH effect at helium temperatures in the semiconducting alloys $\text{Bi}_{1-x}\text{Sb}_x$ ($0.08 \leq x \leq 0.12$) of n - and p -type respectively with electron impurity density $1.3 \times 10^{17} \text{ cm}^{-3} \leq N_L \leq 8 \times 10^{17} \text{ cm}^{-3}$ and with integral impurity hole density $1 \times 10^{17} \text{ cm}^{-3} \leq (P_L + P_T) \leq 2.87 \times 10^{18} \text{ cm}^{-3}$. We determine the angular dependences of the extremal sections S_{extr} (9) of the electron and hole Fermi surfaces in L and in the hole Fermi surface in T when the magnetic field H is rotated in the binary-bisector ($H \perp C_3$) and bisector-trigonal ($H \perp C_2$) planes, with account taken of the motion of the Fermi level in the magnetic field (within the framework of the SBR model²⁶). In the case of complicated oscillation curves, the separation of the frequencies was carried out with the aid of a Fourier analysis with a computer [we used the technique of the rapid Fourier transformation (RFT)³²].

Noticable nonspecularity of the electron and hole spectra in the elongation direction of the equal-energy surfaces in L was observed. It was noted that the anisotropy of the Fermi surface of the electrons and holes at L decreases with increasing Fermi energy; the difference between the anisotropic cross sections and the cyclotron masses increases simultaneously. It is shown that the ratio of the spin and orbit splittings $\gamma = \Delta_s / \Delta_{orb}$ for the maximum section of the Fermi surface at $L(H \parallel C_2)$ approaches unity as $\varepsilon_F \rightarrow 0$. This contradicts the conclusions of Ref. 33 and points to the importance of the Kane interaction ($Q_{22} \neq 0$) in the y direction. For the investigated alloys, we calculated the parameters that enter in the McClure dispersion law.⁹ A comparison with the analogous parameters determined for bismuth^{9, 10, 31} shows that when x is increased in the interval $0-0.1$ the parameter Q_{22} decreases to one-half, the parameters Q_{11} and Q_{33} decrease by less than 10%, while the parameters α_v and α_c remain constant within the limit of errors.

MEASUREMENT PROCEDURE. SAMPLES

We used a setup that made possible automatic recording of the field dependences of the magnetoresistance $\rho(H)$, and also of signals proportional to $\partial\rho/\partial H$ and $\partial^2\rho(H)/\partial H^2$, in magnetic fields up to 60 kOe in the temperature interval $1.9 \text{ K} \leq T \leq 4.2 \text{ K}$, at arbitrary orientations of the magnetic field relative to the crystallographic axes of the investigated single crystals. The SdH oscillations were plotted with an x - y recorder in both the forward and reverse magnetic fields. The current through the superconducting solenoid was set by a current stabilizer with a photoelectric amplifier in the feedback circuit. At a fixed field, the current drift was $\Delta I/I \sim 10^{-4}$ in one hour. The solenoid was calibrated with an NMR magnetometer. The modulation current ($f = 22 \text{ Hz}$) was picked off through a step-down transformer from a TU-100 power amplifier bridged by a deep negative feedback circuit. The maximum modulation current was 15 A, corresponding to a maximum field value $\pm 400 \text{ Oe}$.

A signal proportional to $1/H$ was generated by an analog computing unit based on a Hall pickup with a photoelectric amplifier in the feedback circuit. The sample orientation in the magnetic field was varied by

a drum-type rotating unit. The rotation angle ϑ was measured with a special follow-up system equipped with an inductive pickup. Signals proportional to H , $1/H$, and were fed to digital voltmeters. The accuracy in the determination of H and $1/H$ was $<0.2\%$ and $<1\%$, respectively. The rotation angle ϑ was determined accurately to 0.1° . The current through the samples was carefully stabilized.

In the plots of $\rho(H)$, when necessary, the monotonic variation was suppressed with an analog computing unit based on Hall pickups and generating a signal proportional to $\alpha H \pm \beta H^2$. The difference signal was amplified with an F128 nanovoltmeter. When $\partial\rho(H)/\partial H$ or $\partial^2\rho(H)/\partial H^2$ was plotted, the signal from the potential contacts of the sample was applied to a transistorized narrow-band amplifier with a phase detector tuned to 22 or 44 Hz, respectively. The noise level referred to the input was 5×10^{-9} V. The 44-Hz reference voltage was generated by a frequency doubler.

We investigated the Shubnikov oscillations of the magnetoresistance of 25 single-crystal samples of $\text{Bi}_{1-x}\text{Sb}_x$ ($0.08 \leq x \leq 0.12$) doped with tin, lead (p -type), and tellurium (n -type) (see Table I). The samples were rectangular with characteristic dimensions $\sim 0.8 \times 0.8 \times 4$ mm and were cut from larger single crystals by the electron-spark method. The concentration of antimony in the alloys was determined by chemical analysis accurate ± 0.5 at.%. The current leads were soldered to the end faces of the samples with Wood's alloy, while the potential contacts were electric-spark welded in the central part of the sample spaced ~ 1 mm apart.

EXPERIMENTAL RESULTS

The Shubnikov oscillations of the magnetoresistance were observed at helium temperatures in all the superconducting $\text{Bi}_{1-x}\text{Sb}_x$ ($0.08 \leq x \leq 0.12$) samples, both p - and of n -type, investigated in the present study (see Table I). The oscillation curves were recorded with the magnetic field H rotated in the binary-bisector ($H \perp C_3$)

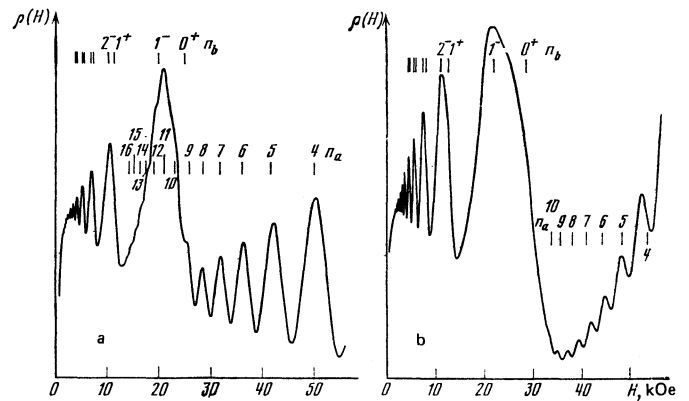


FIG. 1. Oscillations of the longitudinal magnetoresistance ($H \parallel C_2$) at $T = 1.9$ K (the monotonic background is partially suppressed) for the p -type sample 1—1—5 (a) and the n -type sample 2—1—2 (b) of the alloy $\text{Bi}_{0.92}\text{Sb}_{0.08}$ (see Table I). The values of the magnetic field corresponding to the appearance of the Landau quantum levels are marked (calculation by the SBR model,²⁶ see the text).

and bisector-trigonal ($H \perp C_2$) planes. This made it possible to reconstruct in each case the form of the electron (n -type) and hole (p -type) Fermi surfaces in L , and also of the hole Fermi surface in T (p -type).

The cyclotron masses of the electrons and holes on the Fermi level were determined from the temperature dependence of the amplitude of the Shubnikov oscillations at $H \parallel C_2$.^{34, 35} At this orientation we observed in "weak" magnetic fields oscillations from two sections S_b , of equal value and close to the normal section of the two equivalent ellipsoids in L (ellipsoids b). In strong fields we observed oscillations from the maximal section S_a of the third ellipsoid in L (ellipsoid a) (Figs. 1 and 2). The oscillations from S_b and S_a differ in the field because of the strong anisotropy of the Fermi surface in L . We have established that both in the transverse ($H \perp I$) and in the longitudinal ($H \parallel I$) configurations the next Landau

TABLE I. Experimental (E) and theoretical (T) values of the reciprocal periods of the Shubnikov oscillations and of the cyclotron masses in investigations of p - and n -type samples of $\text{Bi}_{1-x}\text{Sb}_x$ at $H \parallel C_2$, as well as the calculated values of the Fermi energy and of the carrier density in L .

x (Type of conductivity)	$\Delta_a^{-1}(H \rightarrow 0)$, kOe		Δ_b^{-1} , kOe		$(m_{ca}/m_0) \cdot 10^4$		$(m_{cb}/m_0) \cdot 10^4$		ϵ_{gL} , MeV	ϵ_{FL} , MeV	$F_L, N_L; 10^{17} \text{ cm}^{-3}$	Sample index
	ϑ	T	ϑ	T	ϑ	T	ϑ	T				
0.08 (p)	33.8±1	34.08	2.3±0.05	2.295	5.9±0.3	6.17	0.44±0.07	0.447	11.5±0.5	8.45	0.232	1-1-1
0.08 (p)	41.7±1	42.4	2.92±0.05	2.91	6.65±0.5	6.64	0.5±0.05	0.495	11.5±0.5	9.95	0.325	1-1-2
0.08 (p)	160.5±2	160.8	12.8±0.4	12.97	10.7±1	10.55	1.04±0.03	0.99	11.5±0.5	26.65	2.63	1-1-3
0.08 (p)	164.3±2	166.3	13.5±0.1	13.49	11.4±0.6	10.7	1.0±0.07	1.0	11.5±0.5	26.25	2.77	1-1-4
0.08 (p)	238±5	250.8	21.8±0.2	21.88	13.0±0.6	12.3	1.3±0.04	1.28	11.5±0.5	34.75	5.35	1-1-5
0.08 (p)	269±4	270.1	24.0±0.1	23.9	14.3±0.7	12.6	1.33±0.04	1.33	11.5±0.5	36.55	6.03	1-1-6
0.08 (n)	182.7±8	192.4	12.0±0.2	11.97	14.0±0.5	13.7	0.97±0.03	0.95	11.5±0.5	24.45	3.1	2-1-1
0.08 (n)	343±10	344.9	23.4±0.2	23.23	17.1±0.5	16.8	1.32±0.02	1.31	11.5±0.5	35.95	7.7	2-1-2
0.08 (n)	343±10	349.3	23.7±0.2	23.57	17.6±0.5	16.9	1.33±0.02	1.32	11.5±0.5	36.25	8.01	2-1-3
0.10 (p)	26.5±1	27.13	1.9±0.05	1.88	5.8±0.4	5.9	0.4±0.04	0.434	14.5±0.5	6.41	0.166	1-2-1
0.10 (p)	53.7±1.5	54.8	3.97±0.1	3.99	7.5±0.9	7.37	0.57±0.05	0.58	14.5±0.5	11.35	0.493	1-2-2
0.10 (p)	89.4±1.5	90.4	6.98±0.05	6.93	8.9±0.3	8.7	0.75±0.03	0.75	14.5±0.5	16.45	1.07	1-2-3
0.10 (p)	159±3	158.3	12.9±0.2	13.14	10.8±0.3	10.5	1.0±0.02	1.0	14.5±0.5	24.65	2.6	1-2-4
0.10 (n)	222.2±9	218	14.05±0.2	14.2	15.0±0.6	14.4	1.03±0.02	1.04	14.5±0.5	25.85	3.83	2-2-1
0.10 (n)	263.1±6	263	17.25±0.2	17.52	15.7±0.6	15.3	1.13±0.03	1.15	14.5±0.5	29.35	5.15	2-2-2
0.10 (n)	296±9	295.5	20.2±0.2	20.0	16.0±0.5	16.0	1.24±0.02	1.23	14.5±0.5	31.75	6.2	2-2-3
0.12 (p)	159.5±5	155.4	13.1±0.2	13.16	10.8±1	10.5	1.01±0.02	1.02	17.5±0.5	23.55	2.55	1-3-1
0.12 (p)	164±5	157.3	13.3±0.1	13.3	10.62±0.3	10.6	1.04±0.02	1.02	17.5±0.5	23.75	2.60	1-3-2
0.12 (p)	186.9±5	190.3	16.17±0.1	16.6	12.3±0.6	11.3	1.1±0.04	1.13	17.5±0.5	27.25	3.52	1-3-3
0.12 (p)	210.4±6	210.1	18.6±0.1	18.62	11.9±0.3	11.6	1.19±0.04	1.20	17.5±0.5	29.25	4.12	1-3-4
0.12 (p)	230.3±5	229.5	20.45±0.2	20.64	13.0±1.5	12.0	1.24±0.08	1.26	17.5±0.5	31.45	4.74	1-3-5
0.12 (n)	110±5	108.4	6.8±0.4	6.87	11.2±0.5	11.3	0.75±0.03	0.76	17.5±0.5	15.35	1.3	2-3-1
0.12 (n)	146.6±5	145.5	9.16±0.2	9.4	11.7±1	12.5	0.82±0.04	0.87	17.5±0.5	18.95	2.05	2-3-2
0.12 (n)	149.1±5	145.5	9.2±0.2	9.4	12.2±0.5	12.5	0.84±0.04	0.87	17.5±0.5	18.95	2.05	2-3-3
0.12 (n)	313.1±10	305.1	21.0±0.4	21.3	16.4±0.5	16.2	1.28±0.02	1.27	17.5±0.5	31.75	6.59	2-3-4

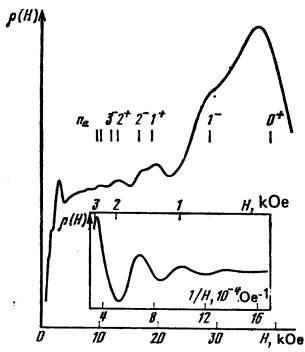


FIG. 2. Oscillations of longitudinal magnetoresistance ($H \parallel I \parallel C_2$) at $T = 1.9$ K (the monotonic course is partially suppressed) for sample 1—1—2 of the p -type alloy $\text{Bi}_{0.92}\text{Sb}_{0.08}$. The values of the magnetic field corresponding to the appearance of the Landau quantum levels (theory) are marked on the figure; the inset shows the low-frequency oscillations from the equivalent ellipsoids b with the monotonic background completely suppressed.

quantum level corresponds to a maximum on $\rho(H)$, in agreement with the results obtained for single-band semiconducting materials of n -type with a simple Fermi surface, such as InSb , InAs , GaSb etc.³⁵⁻³⁷ It is known that the transverse magnetoresistance $\rho(H)$ of pure bismuth passes through a minimum under similar circumstances.³⁴ The difference between the phases of the oscillations of pure bismuth and of the doped semiconducting alloys $\text{Bi}_{1-x}\text{Sb}_x$ is due to the difference between the contributions of the Hall mobility $\sigma_{xy}(H \parallel z)$ to the transverse magnetoresistance in a strong magnetic field:

$$\rho_{\perp} = \sigma_{xy} / (\sigma_{xx}^2 + \sigma_{xy}^2).$$

In pure bismuth, in view of the equality of the electron and hole densities ($N = P$) in a strong field we have $\sigma_{xy} \ll \sigma_{xx}$ and $\rho_{\perp} \sim \sigma_{xx}^{-1}$. In the semiconducting alloys $\text{Bi}_{1-x}\text{Sb}_x$ at helium temperatures there are present either electrons or holes (depending on the type of dopant), so that $\sigma_{xy} \gg \sigma_{xx}$ and $\rho_{\perp} \sim \sigma_{xx}$.

It is difficult to compare the cases of longitudinal magnetoresistance $\rho_{\parallel}(H \parallel I \parallel C_2)$ in Bi and in the semiconducting alloys $\text{Bi}_{1-x}\text{Sb}_x$, inasmuch as the amplitude of the Shubnikov oscillations of ρ_{\parallel} in Bi has an anomalous temperature dependence—it decreases with decreasing temperature. We note only that in all the $\text{Bi}_{1-x}\text{Sb}_x$ alloys investigated by us, both of the n - and p -type, the amplitudes of the oscillations of ρ_{\perp} and ρ_{\parallel} increased with decreasing temperature in accordance with the same law.³⁵

For the small section S_b of the investigated p - and n -type samples, the quantum-limit field corresponding to the doublet ($n_b = 1^-$, $n_b = 0^+$) had a value in the range $1.9 \text{ kOe} \leq H_{qu b} \leq 24 \text{ kOe}$. For samples 1—1—5 (p -type), 2—1—2 (n -type), and 1—1—2 (p -type) of the $\text{Bi}_{0.92}\text{Sb}_{0.08}$ alloy, the values of $H_{qu b}$ at $H \parallel I \parallel C_2$ were respectively 21.1 (Fig. 1a), 22.3 (Fig. 1b), and 2.9 (Fig. 2) kOe. Comparison with Table I shows that these values of $H_{qu b}$ agree within 5% with the oscillation frequency in the reciprocal field Δ_b^{-1} from the small sections S_b . The foregoing result is clearly illustrated by the experimental plots, as functions of $1/H$, of the quantum

number n_b , of the maxima of the series of oscillation peaks from S_b in the investigated alloys. Extrapolation of the linear dependence $n_b(1/H)$ to the value $1/H = 0$ yields $(n_b)_0 \approx -1$ in all cases; this is possible, as seen from the dispersion relation (2), at $\gamma_b \approx 1$. Thus, just as for pure Bi,²⁶⁻³⁰ the ratio γ of the spin and orbital splitting for small sections of the Fermi surface of the semiconducting alloys $\text{Bi}_{1-x}\text{Sb}_x$ in L is close to unity. A more detailed description of the value of γ will be presented below.

It should be noted that at present there is only one theoretical paper³⁸ containing a consistent calculation of the galvanomagnetic tensor of Bi in a quantizing magnetic field at low temperatures on the basis of dispersion relation (2). The expressions for the components of the galvanomagnetic tensor of Bi, obtained in Ref. 38, were intended for computer calculations and cannot be used directly for an analysis of the experiment data. We propose therefore that in fields far from the quantum limit ($\epsilon_F = \text{const}$), the expressions that are valid for each series of oscillation peaks correspond to a definite section of the Fermi surface, are those given in Ref. 35 and obtained for a standard band. Favoring this assumption is a comparison of the experimental and theoretical oscillation curves $\rho_{\parallel}(H)$ at $H \parallel C_2$ carried out for Bi by Brown.³⁴ For a standard band at $\hbar\omega_c \ll \epsilon_F$ and $kT \ll \epsilon_F$ the oscillatory part of the longitudinal magnetoresistance can be represented in the form³⁵

$$(\rho_{\parallel})_{osc} \approx \rho_0 \sum_{r=1}^{\infty} b_r \cos\left(\frac{2\pi\epsilon_F}{\hbar\omega_c} r - \frac{\pi}{4}\right), \quad (3)$$

where $\rho_0 = m^*/Ne^2\tau_0$ is the resistance in a zero magnetic field, b_r is the amplitude of the harmonic r :

$$b_r = \frac{(-1)^r}{r^{3/2}} \left(\frac{\hbar\omega_c}{2\epsilon_F}\right)^{1/2} \frac{2\pi^2 r k T}{\hbar\omega_c} \exp\left(-\frac{2\pi^2 r k T}{\hbar\omega_c}\right) \frac{\cos \pi \gamma r}{\text{sh}(2\pi^2 r k T / \hbar\omega_c)},$$

T_D is the Dingle temperature,³⁹ and $\gamma = m_o/m_s$ is the ratio of the spin and orbital splitting.²⁷ The quantity $(\rho_{\perp})_{osc}$ differs from $(\rho_{\parallel})_{osc}$ by a constant factor and a small oscillating increment which can be neglected in most cases.³⁵

The Shubnikov oscillations from the small section $S_b(H \parallel C_2)$ of all the investigated samples, in the initial interval of magnetic fields ($\hbar\omega_c \ll \epsilon_F$), represented in fact the fundamental frequency ($r=1$) in expression (3); the contribution of the harmonics ($r=2, 3, \dots$) is significant only near the quantum limit for S_b (see Fig. 1 and the inset of Fig. 2). The value of the small cyclotron mass m_{ob} corresponding to S_b , as well as the Dingle temperature T_{Db} , were calculated with a computer from the temperature and field dependences of the amplitude b_1 [see (3)] of the fundamental frequency in fields far from the quantum-limit field $H_{qu b}$. In the course of plotting of the oscillations in the initial section of the magnetic fields, particular attention was paid to suppression of the monotonic behavior of $\rho(H)$ by using an analog computer. The importance of this procedure can be easily understood from a comparison of the oscillation curves in fields up to 3 kOe ($H \parallel I \parallel C_2$) of the sample 1—1—2, plotted with partial (Fig. 2) and total (Fig. 2, inset) compensation of the monotonic variation.

The calculations have shown that in the temperature

interval $1.9 \text{ K} \leq T \leq 4.2 \text{ K}$ the Dingle temperature T_{D_b} corresponding to the oscillations from S_b is a constant. T_{D_b} of samples of either the p - or the n -type was 2.5–3.5 K and did not depend explicitly on the concentration of the impurity carriers in the investigated intervals of the electron and hole densities N and P . To establish the dependence of T_{D_b} on N and P it is necessary to carry out more accurate and more detailed investigations in a larger impurity-carrier density interval.

The values of the small cyclotron mass $m_{ca}(\mathbf{H} \parallel C_2)$ on the Fermi level, calculated in a longitudinal ($\mathbf{H} \parallel \mathbf{I}$) and transverse ($\mathbf{H} \perp \mathbf{I}$) configurations, agreed within the limits of errors. At the same time, a noticeable increase of m_{ca} with increasing S_b was observed (Table I) for alloys of both n - and p -type, thus pointing to a strong nonparabolicity of the electron and hole spectra in L .

The value of the small section S_b can be easily obtained from the relation^{40,41}

$$S_b = \frac{eh}{c} \Delta_b^{-1},$$

where Δ_b^{-1} is the frequency of the Shubnikov oscillations in the reciprocal field. This relation is valid at $\varepsilon_F = \text{const}$ and cannot be directly used in the calculation of the maximal section $S_a(\mathbf{H} \parallel C_2)$ of the hole surface, and particularly the electron Fermi surface in L , since the oscillations from S_a of the investigated $\text{Bi}_{1-x}\text{Sb}_x$ alloys are observed in magnetic-field regions comparable with the quantum-limit field H_b for the small sections S_b (Figs. 1 and 2). In the latter case the dependence of ε_F on the magnetic field H leads to a frequency modulation of the high-frequency oscillations from S_a , and this modulation is particularly strong in the case of semiconducting alloys of n -type, where the stabilization of ε_F by the heavy holes in T (Ref. 13) is completely absent.

The calculations performed in the present study have shown that in the alloys $\text{Bi}_{0.92}\text{Sb}_{0.08}$ and $\text{Bi}_{0.9}\text{Sb}_{0.1}$ the type of the valence band T is respectively 5 ± 1 and 2.5 ± 1 meV lower than the top of the valence band in L (see also Ref. 22). Thus, for alloys with $x \sim 0.1$ the shift of the Fermi level into the interior of the valence band with the aid of an acceptor impurity leads to the appearance of light holes in L , and heavy holes in T . The large state density in the T -extremum contributes to stabilization of ε_F in a strong magnetic field.

The "true" frequency $\Delta_a^{-1}(H \rightarrow 0)$, from which the value of the maximal section is determined

$$S_a = \frac{eh}{c} \Delta_a^{-1}(H \rightarrow 0),$$

was determined in the present study with the aid of computer calculations similar to the SBR calculations²⁶ for pure bismuth. The accuracy of such calculations depends strongly on the number of oscillation peaks registered in the experiment. To obtain the maximum possible number of oscillation periods we recorded simultaneously in the present study the field dependences of $\rho(H)$, $\partial\rho(H)/\partial H$, and $\partial^2\rho(H)/\partial H^2$ at $T = 1.9 \text{ K}$. For n -type samples, the region of magnetic fields in which high-frequency oscillations were observed on $\partial^2\rho(H)/\partial H^2$,

almost doubled in comparison with $\rho(H)$.

The quantum-limit field H_{qa} for the maximum section was observed in the present study only for some of the p -type samples, with light-hole density $P_L < 5 \times 10^{16} \text{ cm}^{-3}$ in L (Fig. 2) (the maximum field attainable with the superconducting solenoid employed by us was $\sim 60 \text{ kOe}$). It should be noted that owing to the motion of the Fermi level in the magnetic field, the phase of high-frequency oscillations determined with the aid of extrapolation of the $n_a(1/H)$ dependence to the value $1/H = 0$ cannot be used for a reliable estimate of the ratio γ_a of the spin and orbital splitting for the maximum section S_a .

The maximum cyclotron mass m_{ca} , as well as the Dingle temperature T_{Da} , was determined from the temperature and field dependences of the amplitude b_1 [see (3)] of the high-frequency oscillations of $\rho(H)$ at $\mathbf{H} \parallel C_2$. The value of T_{Da} (just as of T_{Db}) of the investigated samples of p -type alloys was in the interval 2.5–3.5 K. T_{Da} of n -type alloys was 5–6 K. A comparison of T_{Da} and T_{Db} allows us to conclude that at helium temperatures the anisotropy of the carrier relaxation time in L is small for doped semiconducting $\text{Bi}_{1-x}\text{Sb}_x$ alloys; this contradicts the conclusions of Ref. 8.

The cyclotron mass $m_{ca}(\mathbf{H} \parallel C_2)$ on the Fermi level of p -type alloys was independent, within the limits of experimental error, of the magnetic field H . At the same time, m_{ca} of n -type alloys decreased systematically with increasing magnetic field in the region $H > H_{qa}$, owing to the decrease of ε_F in the magnetic field. The largest change of m_{ca} in a magnetic field registered in the experiment for n -type alloys was 15–20%, which exceeds the error in the measurement of m_{ca} by two or three times. In view of the explicit dependence of m_{ca} on H in n -type alloys, it became necessary to determine the value of m_{ca} corresponding to $\varepsilon_F(H \rightarrow 0)$. This problem, just as the problem of determining the "true" frequency $\Delta_a^{-1}(H \rightarrow 0)$, was solved by the computer calculation of the function $\varepsilon_F(H)$ in the SBR model.²⁶ Similar calculations were carried out to determine the angular dependence of the extremal section of the Fermi surface in L when \mathbf{H} is rotated in the binary-bisector plane in the angle interval $\pm 15^\circ$ relative to the binary direction.

Observation of effects connected with spin splitting^{23, 26–30} encountered difficulties in the present study, owing to the relatively strong scattering by the static defects ($2.5 \text{ K} \leq T_D \leq 3.5 \text{ K}$), as a result of which the fine structure was not very distinct on the oscillation curves even at the lowest temperatures. Nonetheless, at $\mathbf{H} \perp C_3$ we registered reliably the spin-damping-induced doubling of the frequency of the oscillations near the binary direction.²³ The measurements have shown that the spin-damping angle $\vartheta^* = \vartheta(\mathbf{H}, C_2)$ for both p - and n -type alloys depends strongly on the Fermi energy. ϑ^* of p -type alloys ranges from $\pm (3.7 \pm 0.1)^\circ$ at $\varepsilon_{FL} = 36.5 \text{ meV}$ (sample 1–1–6, Table I) to zero at $\varepsilon_{FL} = 11.3 \text{ meV}$ (sample 1–2–2, Table I). At lower values of ε_F , in a narrow angle interval near the binary direction ($\mathbf{H} \parallel C_2$), a splitting of the oscillation peaks, connected with the spin splitting, was observed on the $\rho(H)$ curve (Fig. 2). The maxima on $\rho(H)$ which correspond to appearance of

Landau levels with opposite spin orientation, gradually approached each other with decreasing ε_{FL} . This can be attributed in principle to the approach of $\gamma_a = \Delta_g / \Delta_{orb}$ to unity for the maximum cross section S_a of the Fermi surface in L . This conclusion patently contradicts the results of calculations³³ based on the theory of Abrikosov and Fal'kovskii.⁶

The maximum value of $\vartheta^* = \pm(4.3 \pm 0.1)^\circ$ was registered for sample 2-1-3 of the n -type $\text{Bi}_{0.92}\text{Sb}_{0.08}$ alloy with $\varepsilon_{FL} = 36.2$ meV. At equal values of ε_{FL} and ε_{gL} , the spin-damping angle ϑ^* of n -type alloy always exceeded ϑ^* of p -type alloys.

The Shubnikov oscillations from the holes in T were observed for all investigated p -type alloys. The angular dependence of the extremal section of the hole Fermi surface in T was in full agreement with the results obtained for bismuth doped with acceptor impurities.³¹

DISCUSSION OF RESULTS

In the calculation of the motion of the Fermi level ε_{FL} in the investigated samples in a magnetic field H we used the condition that the carrier density is constant; for n - and p -type alloys this condition takes the respective forms

$$\sum_{i=1}^2 N_i(\varepsilon_{FL}) = N_L = \text{const},$$

and

$$P_T(\varepsilon_{FL} + \Delta) + \sum_{i=1}^2 P_i(\varepsilon_{FL}) = P_T + P_L = \text{const},$$

where N_i and P_i are the concentrations of the electrons and holes in the i th ellipsoid in L , N_L and P_L are the integral concentrations of the electrons and holes in L , and Δ is the energy gap between the tops of the valence bands in L and T , and varies with increasing x .

For the electron density N_i in the i th ellipsoid at $T=0$ we get from (2) the expression²⁶

$$N_i(\varepsilon_{FL}) = \frac{2^{3/2} e H}{h^2 c} (m_i^*)^{3/2} \quad (4)$$

$$\times \sum_{n,s} \left\{ \varepsilon_{FL} \left(1 + \frac{\varepsilon_{FL}}{\varepsilon_{gL}} \right) - \varepsilon(n, s) \right\}^{1/2},$$

where $\varepsilon(n, s) = (n + \frac{1}{2} + \frac{1}{2} s \gamma) \hbar \omega_c$, and ε_{FL} is the Fermi energy reckoned from the bottom of the conduction band. A similar expression holds for the hole density P_i . In the latter case, the Fermi energy is reckoned from the top of the valence band in L (downward on the energy scale).

In contrast to the SBR study,²⁶ where the energy spectrum of the holes in T was described by an ellipsoidal parabolic model, in the present paper we assume for T the model of two interacting bands separated by a direct gap $\varepsilon_{gT} = 200$ meV.³¹ Thus, the hole density P_T is also obtained from (4) by replacing ε_{gL} by ε_{gT} and ε_{FL} by $\varepsilon_{FT} = \varepsilon_{FL} + \Delta$. The values of m_{cT}^* and $m_{\parallel T}^*$ used in (4) for the holes in T were taken from Ref. 31 (see Table II). The values of the parameter γ_T were taken from Ref. 26. The applicability of the two-band model for holes in T (at any rate, in the energy interval $0 < \varepsilon_{FT} < 90$ meV), was demonstrated in Ref. 31. It was shown there also that γ_T does not depend on the energy in the indicated interval.

The calculations of $\varepsilon_F(H)$ in the investigated samples were made mainly for the angle interval $\pm 15^\circ$ about the binary direction ($H \parallel C_2$), in which the frequency modulation of the "high-frequency" oscillations manifests itself most strongly (see Figs. 3-5). The gap ε_{gL} was determined from the dependence of $\varepsilon_{gL}(x)$ obtained in Ref. 3 with the aid of magneto-optical measurements (Table I). The Fermi energy $\varepsilon_F(0)$ in a zero magnetic field was calculated from the values of m_{cb} , Δ_b^{-1} , and ε_{gL} with the aid of the relation

$$\varepsilon_{FL}(0) = \frac{e \hbar}{m_{cb} c} \Delta_b^{-1} - \frac{\varepsilon_{gL}}{2} + \left[\left(\frac{\varepsilon_{gL}}{2} \right)^2 + \left(\frac{e \hbar}{m_{cb} c} \Delta_b^{-1} \right)^2 \right]^{1/2}, \quad (5)$$

which, as follows from (1), is satisfied with good accuracy for sections close to minimal. In the subsequent

TABLE II. Parameters used for the calculation of the motion of the Fermi level in a magnetic field for a number of samples of $\text{Bi}_{1-x}\text{Sb}_x$ alloys of p - and n -type at $H \parallel C_2$ within the framework of the model of Smith, Baraff, and Rowell.²⁶

Parameter	Sample			
	1-1-2, p -type	1-1-3, p -type	1-1-6, p -type	2-1-2, n -type
$P_L, N_L, 10^{17} \text{ cm}^{-3}$	0.32	2.63	5.90	7.50
$\varepsilon_{FL}(0), \text{ MeV}$	9.95	25.8	36.6	36.0
$(m_{ca}^*/m_0) \cdot 10^2$	2.63	2.36	2.02	2.67
$(m_{\parallel a}^*/m_0) \cdot 10^2$	0.126	0.130	0.125	0.126
γ_a	0.7	<0.5	<0.5	<0.5
$(m_{cb}^*/m_0) \cdot 10^2$	0.184	0.188	0.181	0.182
$(m_{\parallel b}^*/m_0) \cdot 10^2$	25.4	20.3	15.7	26.9
γ_b	0.9	0.9	0.8	0.8
$\varepsilon_{gL}, \text{ MeV}$	11.5	11.5	11.5	11.5
$P_T, 10^{17} \text{ cm}^{-3}$	4.14	13.8	22.8	-
$\varepsilon_{FT}(0), \text{ MeV}$	15.0	30.8	41.6	-
$(m_{cT}^*/m_0) \cdot 10^2$	18.8	18.8	18.8	-
$(m_{\parallel T}^*/m_0) \cdot 10^2$	5.7	5.7	5.7	-
γ_T	0.14	0.14	0.14	-
$\varepsilon_{gT}, \text{ MeV}$	200	200	200	-

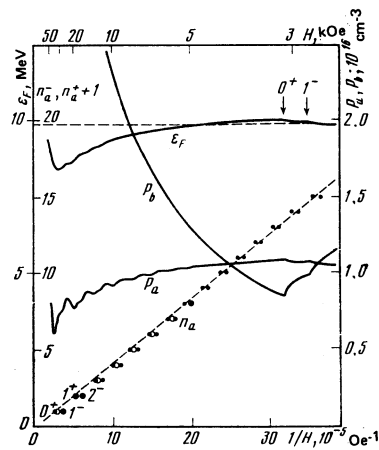


FIG. 3. Field dependences of the energy ε_F and of the hole density P_a in the a ellipsoid, of the hole density P_b in each of the equivalent b ellipsoids and of the quantum numbers (n_a^+, n_a^-) of the oscillations from the ellipsoid a (1—experiment, 2—theory), calculated in the SBR model²⁶ for sample 1-1-2. The dashed lines correspond to the condition $\varepsilon_F = \text{const}$.

calculations of $\varepsilon_{FL}(H)$, the value $\varepsilon_{FL}(0)$ determined from (5) was not varied.

Before we report the results of the calculations, a few remarks are in order. The dispersion relation (2) is not rigorous even when account is taken of the energy dependence of the components of the tensors \hat{m}^* and \hat{m}_s^* introduced by Baraff³⁰ [see (2)]. There is no doubt that the variation of the components of \hat{m}^* with increasing energy leads, in principle, to a dependence of the anisotropy of the low-energy surface on the energy, in agreement with (1). At the same time, the tensor form of the cyclotron mass in (2) excludes the possibility of non-ellipsoidality, which is also contained in (1), and leads in particular to a discrepancy between the anisotropies of the cyclotron masses and the cross sections at sufficiently large ε_{FL} . It will be made clear below that for $\text{Bi}_{1-x}\text{Sb}_x$ alloys (as well as for pure bismuth) the corrections for the interaction with the remote bands in the direction of the short semi-axes of the equal-energy surface in L are of importance only for effects connected with spin splitting, and can be omitted in the remaining cases. In this sense the dispersion relations (1) and (2) are in good agreement.

At the same time, for those orientations of the magnetic field H at which the direction of elongation plays an essential role, the logical connection between (1) and (2) no longer holds. As a result, in particular, at large ε_{FL} it becomes impossible to fit to the experimental data the maximum section $S_{\max} \equiv S_a$ and the maximum cyclotron mass on the Fermi level, $m_{c \max} \equiv m_{ca}$, on the basis of the spectrum (2). Thus, in the case of pure bismuth the value of S_{\max} that follows from the SBR calculations²⁶ is in excellent agreement with analogous value determined by Édel'man¹¹ at $\varepsilon_{FL} \gg \hbar\omega_c$ (i.e., in sufficiently weak fields), whereas the value of $m_{c \max}$ used in Ref. 26 is 7% higher than the true value.¹¹ It is clear therefore that it is particularly important to determine the cyclotron mass on the Fermi level in

the case of large sections by an independent method from experiment.

Baraff has shown³⁰ that in a magnetic field the motion of the Landau 0^- levels that determine the bottom of the conduction band and the top of the valence band is not described by expression (2) and is either linear ($\gamma < 1$, the thermal gap increases in the magnetic field), or hyperbolic ($\gamma > 1$, the thermal gap decreases in the field). Favoring this conclusion are the experimental results given in Refs. 42–44. Estimates show, however, that the calculation of $\varepsilon_{FL}(H)$ only on the basis of the relation (2), in fields that do not exceed considerably the quantum-limit field H for small sections, does not lead to large errors.

In the present paper the calculations of $\varepsilon_{FL}(H)$ were performed for $T=0$. The experimental curves with which the comparison was made were obtained at $T=1.9$ K (Figs. 1 and 2). The thermal smearing of the Fermi level in the latter case did not exceed 0.2 meV, and was much less than ε_{FL} for all the investigated samples (see Table I). In the temperature interval $1.9 \text{ K} < T < 4.2 \text{ K}$, the phase of the oscillations was independent of temperature. It is clear therefore that allowance for the thermal effect in the calculation of $\varepsilon_{FL}(H)$ is not obligatory in our case.

The measurements have shown that in the investigated alloys of n - and p -type the angle φ between the equal-energy surfaces in L and the basal plane is $\varphi = (5 \pm 0.5)^\circ$ (see Fig. 6), somewhat less than for pure bismuth¹¹ ($\varphi_{\text{Bi}} = 6.3^\circ$).¹¹ The minimum cyclotron mass on the Fermi level $m_{c \min}$, which is needed for the calculations, was obtained by multiplying m_{cb} (Table II) by the coefficient $\cos 30^\circ \times \cos 5^\circ = 0.863$.

The maximum cyclotron mass at the bottom of the band was calculated from $m_{c \min}$ with the aid of the relation²⁶

$$m_{c \max} = \frac{m_{c \min}}{1 + 2\varepsilon_{FL}(0)/\varepsilon_{aL}}$$

The theoretical field dependences of the quantum numbers of the oscillations were fitted to the experimental relations (Figs. 1–5) by varying the components of the

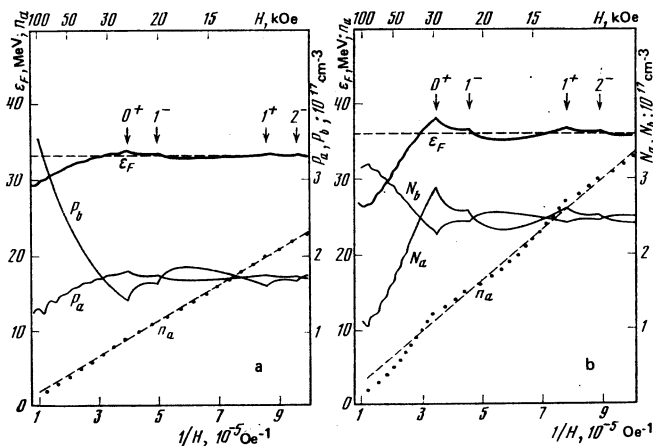


FIG. 4. Field dependences of the Fermi energy ε_F , of the carrier density (P_a, N_a) in ellipsoid a , of the carrier density (P_b, N_b) in each of the equivalent ellipsoids b , and of the quantum numbers n_a of the high-frequency oscillations from the ellipsoid a (without allowance for the spin splitting) at $H \parallel C_2$ in samples of the alloy $\text{Bi}_{0.92}\text{Sb}_{0.08}$: a) sample 1—1—5, p -type; b) sample 2—1—2, n -type. Calculation by the SBR model.²⁶ The dashed lines correspond to the condition $\varepsilon_F = \text{const}$.

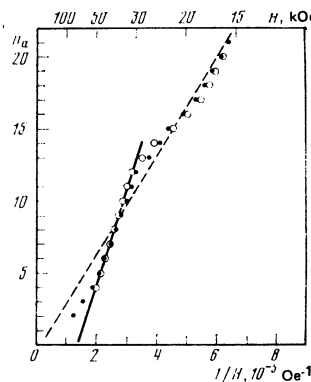


FIG. 5. Field dependences of the quantum number of the high-frequency oscillations from the ellipsoid a (without allowance for the spin splitting) at $H \parallel C_2$ for the sample of the alloy $\text{Bi}_{0.92}\text{Sb}_{0.08}$ (2—1—2): \circ —experiment, \bullet —theory. The dashed line corresponds to the condition $\varepsilon_F = \text{const}$.

effective-mass tensor \hat{m}^* and the values of γ for each sample separately. The values of the parameters used in the calculations for a number of samples at $H \parallel C_2$ are listed in Table II. Examples of calculations of the field dependences of the Fermi energy ε_{FL} , of the quantum number n_a , of the high-frequency oscillations of the maximum section S_a , on the carrier density (P_a, N_a) in the a ellipsoid, and on the carrier density (P_b, N_b) in each of the two equivalent b ellipsoids at $H \parallel C_2$ and $T = 0$ are given in Figs. 3–5 for a number of samples of the $\text{Bi}_{0.92}\text{Sb}_{0.08}$ alloy of p - and n -type.

It is seen from Table II that the values of the small cyclotron mass m_{cb}^* at the bottom of the band, and the values of the small transport mass m_{1a}^* in the direction of the magnetic field are independent, within the limits of errors, of the Fermi energy and are the same for p - and n -type samples. At the same time, the values of the maximum cyclotron mass at the bottom of the band m_{ca}^* and of the transport mass m_{1b}^* increase, in accordance with the conclusions of Ref. 30, with decreasing Fermi energy (thus, as $\varepsilon_{FL} \rightarrow 0$ the anisotropy of the equal-energy surfaces in L increases). At the same Fermi energy, for samples of n -type, the quantities m_{ca}^* and m_{1b}^* are larger than for samples of p -type. The presented data point to the need for taking into account the corrections for the interaction with the remote bands in the elongation direction y [see (1)].

Inasmuch as on the $\rho(H)$ curve there is no splitting of the maxima corresponding to the oscillations from S_b (Fig. 1), the direct calculation of the deviation of γ_b from unity was impossible in the present study. It was

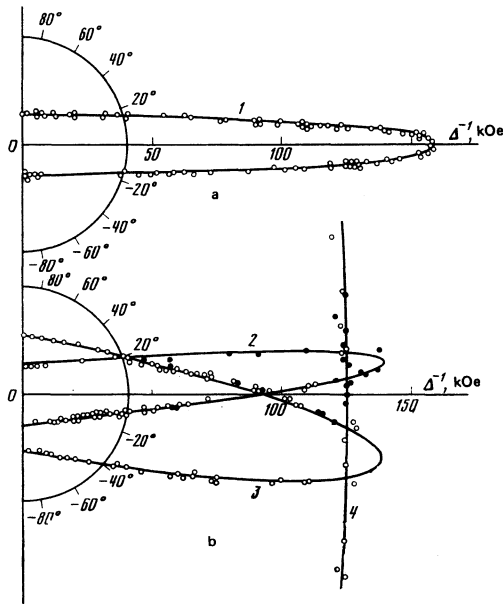


FIG. 6. Angular dependences of the reciprocal period of the Shubnikov oscillations $\Delta^{-1}(H \rightarrow 0) \propto S_{\text{ext}}$, for rotation of the magnetic field in the binary-bisector plane (a) and in the bisector-trigonal plane (b) for sample 1–2–4 of the p -type alloy $\text{Bi}_{0.9}\text{Sb}_{0.1}$. Branches 1–3 pertain to the hole ellipsoids in L , branch 4 pertains to the hole ellipsoid in T . The solid curves are drawn in accord with the ellipsoidal model. In case (a), the angle $\vartheta = 0$ at $H \parallel C_2$, in case (b) the angle $\vartheta = 0$ $H \parallel C_3$. The dark points are the results of a computer Fourier analysis.

established, however, that the character of the $n_a(1/H)$ dependences (Figs. 3–5) changes noticeably when γ_b deviates from unity in fields $\sim H_{qu}$. In particular, the width of the inflection on $n_a(1/H)$ increases when the peaks on the $\varepsilon_{FL}(1/H)$ curve, which correspond to the appearance of the levels $n_b = 1^-$ and $n_b = 0^+$, become spread out. Fitting the theoretical relation $n_a(1/H)$ to the experimental one (Fig. 5) made it possible to determine the value of γ_b with accuracy ± 0.1 (Table II). It should be noted that in the present study it was difficult to distinguish between the cases $\gamma_b = 1 - \delta$ and $\gamma_b = 1 + \delta$. The choice of the values $\gamma_b < 1$ was motivated by the fact that for $\text{Bi}_{1-x}\text{Sb}_x$ alloys with $\varepsilon_{FL} > 0$, the thermal gap in L increases in a magnetic field at orientations of H near the elongation direction, as shown by the results of experimental^{43,44} and theoretical³³ investigations.

The drastic decrease of the spin-damping angle ϑ^* with decreasing Fermi energy, observed in the present study, agrees with the results obtained on the semi-metallic alloys $\text{Bi}_{1-x}\text{Sb}_x$,^{45,46} and can be attributed to the approach of γ_a to unity as $\varepsilon_{FL} \rightarrow 0$. Direct calculations for the p -type samples 1–1–2 ($\varepsilon_{FL} = 9.90$ meV) and 1–2–1 ($\varepsilon_{FL} = 6.40$ meV) yielded the respective values $\gamma_a = 0.7$ (or 1.3) and $\gamma_a = 0.8$ (or 1.2) (Fig. 3). It was impossible in our study to distinguish between the cases $\gamma_a > 1$ and $\gamma_a < 1$, so that the choice $\gamma_1 < 1$ in Table II is arbitrary.

It follows from the theoretical calculations^{28,30,33} that for small sections of the Fermi surface in L we have $\gamma \rightarrow 1$ as $\varepsilon_{FL}, \varepsilon_{gL} \rightarrow 0$. The results obtained by us indicate that an analogous picture is observed also for γ_a corresponding to the maximum value of S_a . This conclusion contradicts the calculations with neglect of the Kane interaction in the direction of elongation of the equal-energy surface in L .³³

For the samples with $\varepsilon_{FL} > 20$ meV, for which the spin-damping angle ϑ^* differs noticeably from zero, the high-frequency oscillations from $S_a(H \parallel C_2)$ did not contain the fine structure connected with the spin splitting. In these cases, for convenience in the calculation, γ_a was assumed equal to zero (Figs. 4 and 5).

A comparison of the functions $n_a(1/H)$ obtained for p - and n -type samples of the alloy $\text{Bi}_{0.92}\text{Sb}_{0.08}$ with approximately equal Fermi energy $\varepsilon_{FL}(0)$ (Figs. 4 and 5) makes it possible to estimate the role of the hole T extremum in the stabilization of ε_{FL} in a magnetic field. The Fermi surface of the n -type sample consists only of three electron ellipsoids in L . The oscillations of the Fermi energy ε_{FL} in fields $H < H_{qu}$ and the decrease of ε_{FL} at $H > H_{qu}$ are strongly pronounced in this case (Fig. 4b). Beyond the quantum limit, for the small section S_b , the increase of the state density on the two neighboring 0^- levels corresponding to the b extrema leads to an intense transfer of the electrons from the a extremum to the b extrema. The Fermi energy decreases rapidly in this case, a fact accompanied by a steep increase in the frequency of the oscillations from the ellipsoid a (the Landau quantum levels and the Fermi energy move towards each other in the magnetic field). For n -type samples in fields $H > H_{qu}$, there exists a section on which the frequency of the oscillations (solid line

on Fig. 5) is practically double the "true" frequency that satisfies the condition $\varepsilon_{FL} = \text{const}$ (dashed line in Fig. 5). A doubled frequency is obtained, for example, in the traditional reduction of high-frequency oscillations shown in Fig. 1b. Neglect of the motion of ε_{FL} in the magnetic field can thus lead to an error of $\sim 100\%$. In the present paper the error in the determination of S_a of n -type samples did not exceed 3–4%.

The oscillations of ε_{FL} in p -type samples in a magnetic field, in view of the absence of a T extremum with heavy holes, are much less pronounced (Figs. 3 and 4a). At $H > H_{qu}$, the strong growth of the hole density P_b in the b extrema takes place mainly on account of the transfer of holes from the T extremum with large state density. The comparatively slow decrease of ε_{FL} in this field region causes only a small increase of the frequency of the oscillations from the ellipsoid a , which at worst (for alloys with $x = 0.12$) reaches $\sim 14\%$ of the "true" frequency.

The error in the determination of S_a of p -type alloys amounted to 1–2%. The frequencies of the oscillations $\Delta_a^{-1}(H \rightarrow 0)$, which are proportional to S_a , are given in Table I for the investigated p - and n -type samples.

It was already indicated above that calculation, within the framework of the SBR model, of the cyclotron mass m_{ca} on the Fermi level from the components of the tensor m^* , selected when fitting the theoretical functions $n(1/H)$ to the experimental data, can lead to errors even in the case of small deviations of the shape of the Fermi surface from ellipsoidal. We have observed that for p -type samples the discrepancy between the experimental and theoretical (SBR) model values of m_{ca} increases with increasing ε_{FL} . This was to be expected in principle, since the deviations from ellipsoidality become more noticeable at large ε_{FL} [see (1)].

The cyclotron mass m_{ca} of n -type samples, calculated from the temperature dependence of the amplitude of the Shubnikov oscillations in fields $H > H_{qu}$, decreases with increasing field because of the strong decrease of ε_{FL} (Fig. 4b). The value of m_{ca} corresponding to $\varepsilon_{FL}(0)$ was obtained in this case by extrapolation of the function $m_{ca}(H)$ to the value of the field H at which $\varepsilon_{FL}(H)$

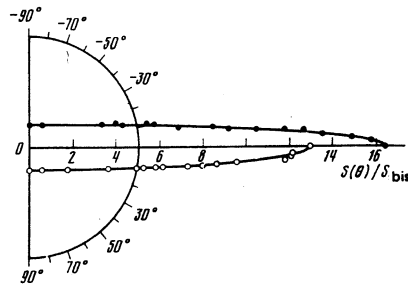


FIG. 7. Dependence of the ratio of the extremal sections $S(\theta)/S_{bis}$ for the hole ellipsoids in L on the angle θ when the magnetic field is rotated in the binary-bisector plane for p -type samples of the alloy $\text{Bi}_{1-x}\text{Sb}_x$: ●—sample 1—1—2, ○—sample 1—1—6. The solid curves were drawn in accord with the ellipsoidal model. The angle $\theta = 0$ at $H \parallel C_2$; S_{bis} —extremal section of the plane perpendicular to the bisector axis through the ellipsoid.

$= \varepsilon_{FL}(0)$ (Fig. 4b). The experimental values of m_{ca} , obtained for the investigated $\text{Bi}_{1-x}\text{Sb}_x$ samples, are given in Table I.

The angular dependences of the sections of the Fermi surface in L at $H \parallel C_3$ and $H \parallel C_2$ agreed for all the investigated p - and n -type samples with the "three-ellipsoid" model (Fig. 6). In the case of strong oscillation curves plotted at $\hbar\omega_c \ll \varepsilon_F$, the frequencies were separated with the aid of a Fourier analysis with a computer³² (dark points on Fig. 6). We have found that for alloys of both the n - and p -type the anisotropy of the Fermi surface in L increases when the bottom (top) of the band is approached (Fig. 7). This effect, which is more strongly pronounced in p -type alloys, contradicts qualitatively the Lax model.

The experimental data obtained in the present study were used for a computer calculation of the parameters that enter in the McClure dispersion law (1). We used in the calculations the expressions obtained by McClure for the principal sections of the Fermi surface in L and for the principal carrier cyclotron masses⁹

$$S_{\min} = \frac{\pi(\varepsilon^2 - \varepsilon_{g1}^2/4)}{Q_{11}Q_{33}}, \quad (6)$$

$$\frac{m_{e \min}}{m_0} = \frac{\varepsilon}{Q_{11}Q_{33}}, \quad (7)$$

$$S_{\max} = \frac{8(\varepsilon^2 - \varepsilon_{g1}^2/4)^{3/2} R^h}{3Q_{33}(\alpha_c \alpha_e)^{1/2}} \left[BE(l) + \left(R - \frac{B}{2}\right) K(l) \right], \quad (8)$$

$$\frac{m_{e \max}}{m_0} = \frac{2\{eK(l) + F[2RE(l) + (B/2 - R)K(l)]\}}{\pi Q_{33}[\alpha_c \alpha_e (\varepsilon^2 - \varepsilon_{g1}^2/4)]^{1/2} R^h}, \quad (9)$$

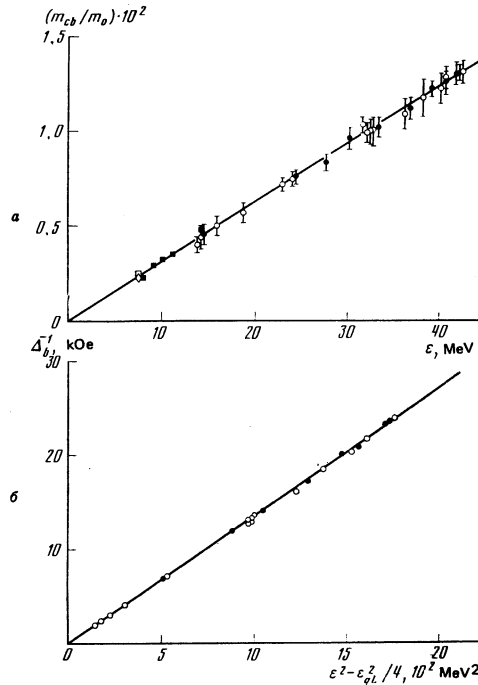


FIG. 8. Plots: a) of the small cyclotron mass m_{cb} against the energy $|\varepsilon| = \varepsilon_F + \varepsilon_{g1}/2$ and b) of the reciprocal period Δ_b^{-1} of the Shubnikov oscillations against $\varepsilon^2 - \varepsilon_{g1}^2/4$ at $H \parallel C_2$ (b ellipsoids for the alloys $\text{Bi}_{1-x}\text{Sb}_x$): ○— p -type alloys (present paper) ●— n -type alloys (present paper), □, ■—data of Refs. 18–20, ◇—from Ref. 17. The solid lines were drawn in accordance with the McClure model with the parameters given in Table III.

$$\frac{S_{\max}}{S_{\min}} = \frac{m_{c \max}}{m_{c \min}} = \frac{Q_{11}}{Q_{33}} \quad (10)$$

where

$$B = -\frac{2Q_{22}^2 + \frac{1}{2}\epsilon_{gL}(\alpha_v + \alpha_c) + \epsilon(\alpha_c - \alpha_v)}{[\alpha_v \alpha_c (\epsilon^2 - \epsilon_{gL}^2/4)]^{1/2}},$$

$$R = (1 + B^2/4)^{1/2},$$

$$F = \frac{(\epsilon^2 - \epsilon_{gL}^2/4)^{1/2} (\alpha_v - \alpha_c)}{2(\alpha_v \alpha_c)^{1/2}},$$

$K(L)$ and $A(L)$ are complete elliptic integrals of the first and second kind, l is the modulus, and

$$l^2 = \frac{1}{2}(B/2 + R)/R.$$

At a given gap ϵ_{gL} we can easily calculate ϵ and $Q_{11}Q_{33}$ with the aid of (6) and (7) from S_{\min} and $m_{c \min}$. The products is factored out into Q_{11} and Q_{33} with the aid of (10). From the energy dependences of S_{\max} and $m_{c \max}$ we can determine for the electrons and holes with the aid of (8) and (9) the values of Q_{22} , α_v , and α_c . The calculation results are given in Tables I and III and in Figs. 8–10. The carrier density (P_L, N_L) contained in Table I was calculated by numerical integration within the framework of the McClure model.

It follows from Fig. 8 that the energy dependences of m_{cb} and Δ_b^{-1} of the investigated p - and n -type alloys agree with (6) and (7). The good agreement of the theory (solid lines on Fig. 8) and the experiment allows us to conclude that in the investigated interval of electron and hole Fermi energies the corrections for the interaction with remote bands in the direction of the short semi-axes of the equal-energy surface in L do not manifest themselves noticeably, and can be omitted (as was done in fact in Ref. 9).

Similar constructions for m_{ca} and $\Delta_a^{-1}(H \rightarrow 0)$, as seen from Fig. 9, leads to qualitatively different (compared with Fig. 8) results. The energy dependences of m_{ca} and $\Delta_a^{-1}(H \rightarrow 0)$ split into two branches (electrons and holes) and are not linear. Thus, the two-band approximation is not suitable in this case. In equally poor agreement with experiment is the simplified ($Q_{22} = 0$) model of Cohen⁵ (or the model of Abrikosov⁸). In Fig. 9 this model is represented by dashed curves calculated for the average gap $\epsilon_{gL} = 14.5$ meV ($x = 0.10$) with the parameters given in Table III. The solid curves are drawn in accordance with the McClure model ($Q_{22} \neq 0$) also for the case of the average gap. It should be noted that the degree of agreement between the theory and experiment cannot be completely estimated from Figs. 9

TABLE III. Values of the parameters that enter in the dispersion law* for the alloys $\text{Bi}_{1-x}\text{Sb}_x$ and for bismuth.

	Q_{11}	Q_{22}	Q_{33}	α_c	α_v
$\text{Bi}_{1-x}\text{Sb}_x$	0.412 ± 0.010	0.016 ± 0.003	0.329 ± 0.010	0.63 ± 0.1	1.00 ± 0.15
0.08 ≤ x < 0.12	0.412	0	0.329	1.15	1.55
Bi	0.465 ± 0.008	0.033 ± 0.002	0.346 ± 0.006	0.80 ± 0.15	1.19 ± 0.20

*First line—parameters entering in the dispersion equation of McClure⁹ for the alloys $\text{Bi}_{1-x}\text{Sb}_x$ in accordance with the data of the present paper; second line—parameters entering in the dispersion equation of Abrikosov and Fal'kovskii. Third line—parameters of the McClure spectrum for bismuth, obtained in Ref. 31 at $\epsilon_{gL} = -9$ meV and $\epsilon = 31$ meV.

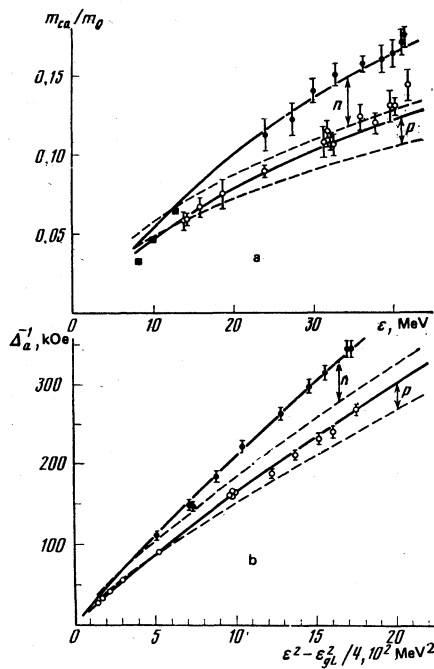


FIG. 9. Plots: a) of the maximum cyclotron mass m_{ca} against the energy $|\epsilon| = \epsilon_F + \epsilon_{gL}/2$ and b) of the reciprocal period $\Delta_a^{-1}(H \rightarrow 0) \propto S_{\max}$ of the Shubnikov oscillations (a ellipsoid) against $\epsilon^2 - \epsilon_{gL}^2/4$ at $H \parallel C_2$ for the alloys $\text{Bi}_{1-x}\text{Sb}_x$: \circ — p -type alloys (present paper); \bullet — n -type alloys (present paper); \blacksquare —from Ref. 20. The solid curves were drawn in accordance with the McClure model for the case $\epsilon_{gL} = 14.5$ meV with the parameters given in Table III. The dashed curves were drawn in accordance with the model of Abrikosov and Fal'kovskii ($Q_{22} = 0$) for the case $\epsilon_{gL} = 14.5$ meV (the corresponding parameters are also contained in Table III).

and 10, since the theoretical curves for the alloys with $x = 0.8$ and $x = 0.12$ are shifted somewhat relative to $x = 0.1$ on account of the difference in ϵ_{gL} . Therefore the comparison of the theoretical and experimental values of m_{ca} and $\Delta_a^{-1}(H \rightarrow 0)$ is best carried out using the data listed in Table I. The fact that the electron and hole

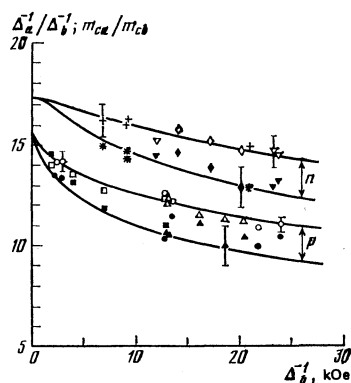


FIG. 10. Plots of the ratios $\Delta_a^{-1}(H \rightarrow 0)/\Delta_b^{-1}$ of the reciprocal periods (light circles and +), and of the corresponding cyclotron masses m_{ca}/m_{cb} (dark points and *) against the small reciprocal period $\Delta_b^{-1}(H \parallel C_2)$ for the investigated superconducting alloys $\text{Bi}_{1-x}\text{Sb}_x$ of n -type (two upper branches) and p -type (two lower branches): \circ, \bullet — $x = 0.08$ (p), \square, \blacksquare — $x = 0.10$ (p), $\triangle, \blacktriangle$ — $x = 0.12$ (p), $\nabla, \blacktriangledown$ — $x = 0.08$ (n), \diamond, \blacklozenge — $x = 0.10$ (n), $+, *$ — $x = 0.12$ (n). The solid curves were drawn in accordance with the McClure model for the case $\epsilon_{gL} = 14.5$ meV.

spectra in L are not mirror images in the y direction is a consequence of the difference between α_v and α_c (see Table III). The deviation of α_v and α_c from zero leads to a divergence of the anisotropies of the sections and of the cyclotron masses with increasing Fermi energy in both the valence and in the conduction band (Fig. 10).

It is of interest to compare the parameters obtained in the present paper for the carrier spectrum in L for the investigated alloys with the parameters determined in Ref. 31 for bismuth. It is seen from Table III that the parameters Q_{11} and Q_{33} decrease with increasing x from 0 to 0.8–0.12 by approximately 10%. The parameters α_c and α_v , when account is taken of the relatively large errors in their determination, most readily remain unchanged. At the same time, the parameter Q_{22} decreases by a factor of 2. The character of the variation of Q_{22} with x remains unclear, however.

In conclusion, the authors use the occasion to express deep gratitude to N. B. Brandt for systematic help with the work and for most helpful discussions of the results.

- ¹N. B. Brandt, Ya. G. Ponomarev, and E. M. Chudinov, *J. Low Temp. Phys.* **8**, 423 (1972).
- ²F. A. Buot, *The Phys. of Semimet. and Narrow-Gap Semicond.*, Proc. Conf., Dallas, eds. D. L. Carter and R. T. Bate, Pergamon Press, 1971, p. 99.
- ³E. J. Tichovol'ski and J. G. Mavroides, *Solid State Commun.* **7**, 927 (1969).
- ⁴B. Lax, *Bull. Am. Phys. Soc.* **5**, 167 (1960).
- ⁵M. H. Cohen, *Phys. Rev.* **121**, 387 (1961).
- ⁶A. A. Abrikosov and L. A. Fal'kovskii, *Zh. Eksp. Teor. Fiz.* **43**, 1089 (1962) [*Sov. Phys. JETP* **16**, 769 (1962)].
- ⁷L. A. Fal'kovskii and G. S. Razina, *Zh. Eksp. Teor. Fiz.* **49**, 265 (1965) [*Sov. Phys. JETP* **22**, 187 (1965)].
- ⁸A. A. Abrikosov, *J. Low Temp. Phys.* **8**, 315 (1972).
- ⁹J. W. McClure, *J. Low Temp. Phys.* **25**, 527 (1976).
- ¹⁰J. W. McClure and K. H. Choi, *Solid State Commun.* **21**, 1015 (1977).
- ¹¹V. S. Édel'man, *Usp. Fiz. Nauk* **123**, 257 (1977) [*Sov. Phys. Usp.* **20**, 819 (1977)].
- ¹²N. B. Brandt, Chan Tchi Ngok Bick, and Ya. G. Ponomarev, *Zh. Eksp. Teor. Fiz.* **72**, 989 (1977) [*Sov. Phys. JETP* **45**, 517 (1977)].
- ¹³E. P. Buyanova, V. V. Evseev, G. A. Ivanov, G. A. Mironova, and Ya. G. Ponomarev, *Fiz. Tverd. Tela (Leningrad)* **20**, 1937 (1978) [*Sov. Phys. Solid State* **20**, 1119 (1978)].
- ¹⁴N. B. Brandt and Ya. G. Ponomarev, *Zh. Eksp. Teor. Fiz.* **55**, 1215 (1968) [*Sov. Phys. JETP* **28**, 635 (1968)].
- ¹⁵V. A. Yastrebova, Author's Abstract of Candidate's Dissertation, Moscow State University, 1974.
- ¹⁶G. A. Antcliffe, *Phys. Lett.* **28A**, 601 (1969).
- ¹⁷N. B. Brandt, V. A. Yastrebova, O. N. Belousova, D. Hesse, and Ya. G. Ponomarev, in: *Polumetal'ly i poluprovodniki z*
- uzkimi zapreshchennymi zonami (Semimetals and Semiconductors with Narrow Forbidden Bands)*, L'vov, 1973, p. 102.
- ¹⁸G. Oelgart and R. Herrmann, *Phys. Status Solidi B* **58**, 181 (1973).
- ¹⁹G. Oelgart and R. Herrmann, *Phys. Status Solidi B* **61**, 137 (1974).
- ²⁰G. Oelgart and R. Herrmann, *Phys. Status Solidi B* **75**, 189 (1976).
- ²¹M. R. Ellett, R. B. Horst, L. R. Williams, and K. F. Cuff, *J. Phys. Soc. Jpn.* **21**, Suppl. 666 (1966).
- ²²L. S. Lerner, K. F. Cuff, and L. R. Williams, *Rev. Mod. Phys.* **40**, 770 (1968).
- ²³N. B. Brandt, T. F. Dolgolenko, and N. N. Stupochenko, *Zh. Eksp. Teor. Fiz.* **45**, 1319 (1963) [*Sov. Phys. JETP* **18**, 908 (1963)].
- ²⁴C. G. Grenier, J. M. Reynolds, and J. R. Sybert, *Phys. Rev.* **132**, 1 (1963).
- ²⁵N. B. Brandt and L. G. Lyubutina, *Zh. Eksp. Teor. Fiz.* **47**, 1711 (1964) [*Sov. Phys. JETP* **20**, 1150 (1964)].
- ²⁶G. E. Smith, G. A. Baraff, and J. W. Rowell, *Phys. Rev. A* **135**, 1118 (1964).
- ²⁷M. H. Cohen and E. J. Blount, *Philos. Mag.* **5**, 115 (1960).
- ²⁸S. Takano and M. Koga, *J. Phys. Soc. Jpn.* **42**, 853 (1977).
- ²⁹K. Tayoda, Y. Sawada, and H. Kawamura, *J. Phys. Soc. Jpn.* **32**, 653 (1972).
- ³⁰G. A. Baraff, *Phys. Rev.* **137**, A842 (1965).
- ³¹R. Muller, Author's Abstract of Candidate's Dissertation, Moscow State University, 1979.
- ³²E. O. Brigham and R. E. Morrow, *IEEE Spectrum* **4**, 63 (1967).
- ³³S. D. Beneslavskii and L. A. Fal'kovskii, *Fiz. Tverd. Tela (Leningrad)* **16**, 1360 (1974) [*Sov. Phys. Solid State* **16**, 876 (1974)].
- ³⁴R. D. Brown III, *Phys. Rev. B* **2**, 928 (1970).
- ³⁵L. M. Roth and P. N. Argyres, *Semiconductors and Semimetals*, eds. R. K. Willardson and A. C. Beer, Vol. 1, Academic Press, New York, 1966, p. 159.
- ³⁶B. M. Askerov, *Kineticheskie éffekty v poluprovodnikakh (Kinetic Effects in Semiconductors)*, Nauka, Leningrad, 1970.
- ³⁷I. M. Tsidil'kovskii, *Zonnaya struktura poluprovodnikov (Band Structure of Semiconductors)*, Nauka, Moscow, 1978.
- ³⁸Y. Way, Y. Kao, and S. Wang, *Phys. Rev. B* **8**, 3500 (1973).
- ³⁹R. B. Dingle, *Proc. Roy. Soc. London Ser. A* **211**, 517 (1952).
- ⁴⁰L. Onsager, *Philos. Mag.* **43**, 1006 (1952).
- ⁴¹I. M. Lifshitz and A. M. Kosevich, *Zh. Eksp. Teor. Fiz.* **29**, 730 (1955) [*Sov. Phys. JETP* **2**, 636 (1955)].
- ⁴²M. P. Vecchi and M. S. Dresselhaus, *Phys. Rev. B* **10**, 771 (1974).
- ⁴³N. B. Brandt, S. M. Chudinov, and V. G. Karavaev, *Zh. Eksp. Teor. Fiz.* **70**, 2296 (1976) [*Sov. Phys. JETP* **43**, 1198 (1976)].
- ⁴⁴N. B. Brandt, B. A. Korchak, and S. M. Chudinov, *Fiz. Nizk. Temp.* **3**, 152 (1977) [*Sov. J. Low Temp. Phys.* **3**, 72 (1977)].
- ⁴⁵S. M. Chudinov, B. A. Akimov, and V. V. Moschalkov, *Fiz. Tverd. Tela (Leningrad)* **17**, 2301 (1975) [*Sov. Phys. Solid State* **17**, 1522 (1975)].
- ⁴⁶B. A. Akimov, Abstract of Candidate's Dissertation Moscow State University, 1975.

Transl. by J. G. Adashko